Neurodegeneration by polyglutamine Atrophin is not rescued by induction of autophagy

Manolis Fanto, Ilaria Nisoli, Jean Paul Chauvin, Francesco Napoletano, Piera Calamita, Valentina Zanin, Bernard Charroux

Neurodegeneration by polyglutamine Atrophin is not rescued by induction of autophagy

Ilaria Nisoli[1], Jean Paul Chauvin[2], Francesco Napoletano[1], Piera Calamita[1], Valentina Zanin[1], Manolis Fanto[1,3*] and Bernard Charroux[2*]

[1] *Dulbecco Telethon Institute and Division of Neuroscience, DIBIT-San Raffaele Scientific Institute, Via Olgettina 58, I-20132 Milan*

[2] *IBDML, Campus de Luminy Case 907, F-13288 Marseille Cedex 9.*

[3] *MRC Centre for Developmental Neurobiology, King's College London, Guy's Campus, London SE1 1UL*

**These authors contributed equally and are co-corresponding authors. Correspondence should be addressed to Bernard Charroux (email: charroux@ibdml.univ-mrs.fr) or to Manolis Fanto (email: manolis.fanto@kcl.ac.uk).*

Running Title: Autophagy deregulation in a DRPLA *Drosophila* model

ABSTRACT

Polyglutamine pathologies are neurodegenerative diseases that manifest both general polyglutamine toxicity and mutant protein specific effects. Dentatorubropallidoluysian Atrophy (DRPLA) is one of these disorders caused by mutations in the Atrophin-1 protein. We have generated several models for DRPLA in *Drosophila* and have analysed the mechanisms of cellular and organism toxicity. Our genetic and ultrastructural analysis of neurodegeneration suggests may play a role in cellular degeneration when polyQ proteins are overexpressed in neuronal and glial cells. Clearance of autophagic organelles is blocked at the lysosomal level after correct fusion between autophagosomes and lysosomes. This leads to accumulation of autofluorecent pigments and of proteinaceous residues usually degraded by the autophagy-lysosome system. In these circumstances, further pharmacological and genetic induction of autophagy does not rescue neurodegeneration by polyQ Atrophins, in contrast to many other neurodegenerative conditions. Our data thus provide a crucial insight into the specific mechanism of a polyglutamine disease and reveal important differences in the role of autophagy with respect to other diseases of the same family.

INTRODUCTION

Polyglutamine (polyQ) pathologies are a family of dominantly inherited neurodegenerative diseases caused by mutations in which an expanded CAG repeat tract results in a long stretch of Qs in the encoded protein. This family includes Huntington Disease, Dentatorubral-pallidoluysian Atrophy (DRPLA) and several spinocerebellar ataxias. Apart from their polyQ repeats, the proteins involved are unrelated, and although they are all widely expressed in the CNS and peripheral tissues, they lead to

distinct patterns of neurodegeneration[1]. PolyQ-expanded proteins misfold and accumulate in large aggregates, which have been initially described as toxic[1], and more recently as a positive prognosis factor in neuronal survival[2]. The molecular and cellular mechanisms of toxicity due to polyQ proteins are not fully characterised yet and many of the key aspects are under intense scrutiny. In particular, many reports have described autophagy as a protective cellular mechanism in neurodegeneration[3], although its full contribution to the pathogenesis, including cell killing, is still poorly understood. The full cycle of autophagic degradation of cellular components and recycle of simpler constituents is not involved in cell killing. However many dysfunctions at different steps of this cycle that have been reported upon expression of toxic proteins, including polyQ proteins, can lead to cell degeneration and death[4].

Over the past few years a growing number of studies have focused at identifying the interplay between polyQ effects and protein-specific misfunctions[5-7], with the assumption that polyQ pathologies combine general polyQ toxicity to disease-specific effects due to the proteins affected. The fruitfly *Drosophila melanogaster* has proved to be a valuable model organism for polyQ diseases and neurodegeneration[8]. New models have also moved on from initial basic observations, revealing the complex interplay between polyQ effects and RNA or protein-specific misfunction[5,7,9].

We generated several *Drosophila* models of DRPLA (Fig. 1a and Supplementary Fig. 1), a polyQ disease caused by mutations in *atrophin-1*[10,11]. Atrophins are transcriptional co-factors conserved from *Drosophila* to mammals[12-15], providing an ideal background for the dissection of polyQ effects and specific Atrophin functions through *Drosophila* genetics. We show that polyQ Atrophins promote neurodegeneration with autophagic hallmarks both in neuronal photoreceptors and glial cells. Through a block of lysosomal digestion they hamper the beneficial effects of further autophagy induction, differently from other proteinopathies. Thus, our data

uncover a specific mechanism of toxicity of a polyglutamine disease and reveal a complex interplay of Atrophins with autophagy.

RESULTS

Retinal degeneration by *Drosophila* Atro and human Atrophin-1

The *Drosophila Atrophin* gene (*Atro*) encodes for a large ubiquitous protein containing all functional domains of Atrophins, including two polyQ stretches[12,14]. We have expanded either stretch to engineer the Atro75QN and the Atro66QC proteins (Fig. 1a and Supplementary Fig. 1). The former carries a 75Q stretch in the middle of a polyprolin domain, in a similar position to where the Q stretch is found in human Atrophin-1 (At-1), whereas the latter carries a 66Q stretch at the C-ter end at a position where there is a Q stretch not conserved with human At-1. Both Atro proteins are able to rescue *Atro* embryonic lethality, albeit with slightly different efficiency (Supplementary Tab. 1), indicating that polyQ expansion does not cause generalised loss of Atro function. Overexpression in the eye with *GMR-Gal4* of Atro75QN or Atro66QC induces progressive depigmentation (Fig. 1b), commonly observed in neurodegenerative models in the eye. In addition, adult expression of Atro using the *Rhodopsin1 (Rh1)* driver is sufficient for degeneration, which is visible in terms of loss of photoreceptor cells specifically due to ageing (Fig. 1c and Supplementary Fig.1). The latter experiment also shows that photoreceptor degeneration is strictly cell autonomous as R7, the only cell that does not express *Rh1-Gal4*, is never lost (Fig. 1c, arrows). With *GMR-Gal4* it is possible to observe, in horizontal head sections, a generalised tissue consumption which leads to dramatic retinal collapse (Fig. 5, see also figure legend). This is specifically observed with ageing as all Atro expressing flies display a correctly sized retina when they eclose from the pupal case (data not shown). In all these assays

Atro75QN results in more severe phenotype despite lower full length expression levels when compared to Atro wt and Atro 66QC (Supplementary Fig.1). Interestingly, Atro wt also induces statistically significant photoreceptor loss and retinal consumption, although at a much lower level than its polyQ counterparts (Fig. 1c and Fig. 5b). This raises the possibility that degeneration induced by polyQ Atro is a combination of polyQ toxicity and detrimental effects of Atro itself.

As previously reported[16], and similarly to fly Atro proteins, a human At-1 fragment with a polyQ expansion (At-1-65QΔC, which accumulates in DRPLA patients and has been shown to be an At-1 form of extreme toxicity[17]) induces progressive eye depigmentation (Fig. 1b) and retinal collapse (Fig. 5c) when expressed in the fly retina. Surprisingly, expression of full length human At-1 does not promote any major degeneration of the fly retina, also when carrying a 65Q tract (Fig. 1b and Fig. 5c). Interestingly, full length At-1, regardless of polyQ length, is expressed at low levels despite normal mRNA expression levels (Supplementary Fig. 1), and this could explain the lack of a dramatic effect in the retina. The mechanism responsible for the low At-1 levels is unknown, but it does not involve protein degradation via the proteasome or macroautophagy (Supplementary Fig. 2). Since the highly expressed ΔC transgenes derive from the full length ones, differential translation efficiency is also unlikely, as they share the very same 5'UTR and beginning of the ORF up to the point of deletion (aa 917).

Finally, intracellular aggregates, a hallmark of polyQ diseases, are formed upon polyQ Atrophins expression (Supplementary Fig. 3). We have analysed in detail those formed by At-1-65QΔC and found that this protein is able to recruit in its heavily ubiquitinated aggregates the endogenous fly Atro; general transcription factors like the TATA-box Binding Protein (TBP); chaperones like Hsp70; Nervy (the *Drosophila* orthologue of Atrophin-1 interactor ETO/MTG8[18]); chromatin modifying enzymes like

the histone deacetylase Rpd3. However the co-repressor Sin3A, often found in the same complex with Rpd3, and Mi-2, part of the NuRD chromatin remodelling complex, are not enriched in aggregates, indicating that these have a specific content rather than being a general protein trap.

Glial cells are particularly sensitive to polyglutamine Atrophins

Neurodegenerative phenotypes in the DRPLA fly models are not restricted to retinal photoreceptors. Neuronal overexpression of fly Atro results in developmental abnormalities[19] that severely affect viability. However, switching polyQ Atro on only during adult life affects fly longevity specifically. Both Atro75QN and Atro66QC are toxic when expressed in the glia (Fig. 2a), albeit at different levels, whereas only Atro75QN is toxic in neurons (Fig. 2b). This suggests that glial cells are particularly sensitive to fly polyQ Atrophins. Also, glial expression does not affect development and the reduction in viability is primarily due to expression in adult life (Fig. 2a,c and Supplementary Fig. 4). Similarly, At-1-65QΔC but not its wt counterpart reduces fly viability if expressed in neurons or in the glia (Fig. 2e,f and Supplementary Fig. 4). Glial expression with two different drivers results in a stronger phenotype than in case of neuronal expression. Interestingly, also the low expressed At-1-65Q reduces significantly fly viability when driven in the glia, but not in neurons (Fig. 2e,f). Under the same conditions, flies expressing a form of human Huntingtin, Htt-exon-1-93Q[20] display on the contrary a faster mortality upon neuronal expression (Supplementary Fig. 4). Thus, our viability assays indicate that polyQ Atrophins are toxic both in neurons and glial cells, with a noticeable sensibility of glial cells specific to polyQ Atrophins.

In conclusions all DRPLA fly models recapitulate typical polyQ toxicity but also suggest that protein-specific effects may modulate the phenotypes in comparison to other polyQ models.

Accumulation of autophagic hallmarks in degenerating neurons and glia.

It has been reported that part of the toxicity exerted by polyQ proteins results from a block in the proteasome[21,22]. However neither *Drosophila* nor human polyQ Atrophins impair proteasome functions extensively (Supplementary Fig. 5). This suggests that although proteasomal impairment may contribute to their phenotype, their toxic effect is unlikely to be due to a massive block of the proteasome.

Overexpression of Atro through mutations in the micro RNA mir8 has been shown to promote apoptosis during larval neuronal development[19]. In aged adult retinae, significant accumulation of TUNEL signal is detected only if polyQ Atrophins are expressed in all eye cells with the *GMR* driver but not when the *Rh1* driver is used to express the Atro proteins specifically in photoreceptor neurons (Supplementary Fig. 5). Although these data confirm that polyQ Atrophins can stimulate apoptosis in developing tissues and non neuronal adult eye cells, apoptosis does not appear to be chiefly responsible for the degeneration of adult postmitotic photoreceptor neurons,. TUNEL signal in fact correlates well with depigmentation, which could be due to apoptotic death of pigment cells.

At a finer level of analysis, electron microscopy (EM) of degenerating photoreceptors reveals that wt Atro promotes the formation of autophagic vacuoles, rarely found in control retinae (Fig. 3a). PolyQ Atrophins induce the formation of innumerable typical autophagosomes that cluster together and fuse with electrondense

lysosomal compartments to form large autophagolysosomes (Fig. 3a). Accumulation of similar autophagic organelles is also found in glial cells expressing polyQ Atrophins just before organism death (Supplementary Fig. 6). In addition, many mitochondria display abnormal morphology, although they are hardly present in strongly degenerated tissue (Fig. 3a). The presence of autophagic organelles is confirmed for Atro66QC and Atro75QN by punctuated staining in the retina for GFP::Atg8a, a marker for autophagy (Fig. 3b)[23]. GFP::Atg8a clustering in Atro wt is present but less substantial, in agreement with the electron microscopy analysis (Fig. 3b).

In conclusion autophagosomes and autophagic markers dramatically accumulate inside cells expressing polyQ Atrophins, suggesting a major role of autophagy in this form of cellular degeneration.

Neurodegeneration is not rescued by further induction of autophagy.

Having established the presence of autophagy, we further analysed its functional significance for neurodegeneration in the DRPLA flies.

Blocking the signalling responsible for autophagy induction[23] by generating mutant clones for *atg1*$^{\Delta 3D}$ (a deletion of 966bp that includes the Atg1 translation start site[23] and thereby a putative null allele) leads to an increase in the degeneration caused by polyQ Atro (Fig. 4a), revealing that endogenous autophagy attempts at protecting from neurodegeneration, as reported in other models. This is confirmed by the enhancement of Atro retinal degeneration following RNAi-mediated downregulation[23] of Atg5, a key autophagy factor (Fig. 5b). *Atg5*^{IR} also enhances fly mortality due to glial expression of polyQ Atrophins (Supplementary Fig. 7). On the contrary, overexpressing the chaperone dHdj1 significantly suppresses polyQ Atro toxicity in both assays (Fig.

5b and data not shown). This indicates that it is possible to rescue the DRPLA flies through another mechanism known to protect from polyQ toxicity and argues for the specificity of the effect observed with *atg5*^{IR}.

Autophagy is controlled by the Tor signalling pathway in response to several stimuli[3] and induction of further autophagy through inhibition of the Tor pathway has been reported to alleviate a number of neurodegenerative conditions[24-27]. However, in our model, expression of a dominant negative form of the Tor kinase, Tor^{TED}, a strong inducer of autophagy[23], enhances retinal degeneration by all Atro forms (Fig. 5b). In addition, Tor^{TED} expression further reduces the vitality of flies expressing At-1-65Q in the glia (Fig. 2d) and results in lethality at larval stages when co-expressed in the glia with At-1-65QΔC and any *Drosophila* Atro form (data not shown). On the contrary, Tor^{TED} has no effect *per se* on viability and longevity if expressed in the glia under the same conditions (Supplementary Fig. 7).

Likewise, the addition in the fly food of 1μM rapamycin, a potent inhibitor of Tor, leads to a significant and highly reproducible decrease in the number of photoreceptor cells per ommatidium in flies expressing Atro75QN (Fig. 4b and Supplementary Tab. 2). Fly development was delayed by approximately 3 days on rapamycin as previously described[23], indicating that the drug is effective in the conditions we used. Flies expressing human Htt-exon-1-93Q treated in parallel under the same conditions display a small rescue (Supplementary Fig. 7). Finally, rapamycin also enhances mortality of flies expressing Atro75QN in the glia with the *repo* driver and heterozygous for the null *Tor*$^{\Delta P}$ mutation (Supplementary Fig.7).

More direct stimulation of autophagy downstream of Tor, by overexpressing the Atg1 gene, brings about an even more dramatic enhancement of retinal degeneration by all Atro forms (Fig. 5b). We have used for this assay a weak UAS-Atg1 stock[28],

obtained by the insertion of the Gene Search transposon GSV6 upstream of the *atg1* gene, whose moderate expression does not affect *per se* retinal consumption (Fig. 5b).

In conclusion our data indicate that although endogenous autophagy plays a crucial role in moderating polyQ Atrophin toxicity, further induction of autophagy does not rescue neurodegeneration of our DRPLA fly models, differently from what has been reported for other *Drosophila* neurodegeneration models[24,27].

Autophagic digestion is blocked at the lysosomal level.

Vacuoles formed upon Atro overexpression appear to be characteristically filled with unstructured partially degraded debris. On the contrary, expression of Tor^{TED} or Atg1 promotes formation of autophagic vacuoles that appear empty (Fig. 3a and Supplementary Fig. 6). In addition, autophagosomes fused with the dark electrondense lysosomes still keep their inner membrane (Fig. 3a), which is normally readily degraded. These structures form when complete digestion of autophagolysosomes has been blocked with lysosomotropic agents[29]. These data therefore suggest that Atro is partially blocking or abnormally delaying autophagy at the level of digestion of autophagosomes.

One possibility to explain the lack of digestion is that autophagosomes are not able to fuse with lysosomes. However, in dissected single ommatidia in culture many GFP::Atg8 punctae, which accumulate upon expression of Atro wt and more strongly upon Atro75QN expression, co-localise with lysotracker-positive compartments (Fig. 6a), indicating that fusion between autophagosomes and lysosomes is functional in these cells and an eventual block of the autophagic flux is subsequent to the formation of autophagolysosomes. Also lysotracker staining indicates correct acidification of

autophagolysosomes. In fact, expression of all forms of Atro elicits massive accumulation of large acidic compartments, positive for lysotracker staining both in adult ommatidia and in imaginal discs (Fig 6a and Supplementary Fig. 8). The small bright dots visible in the red lyostracker channel also in control ommatidia however are an artefact due to pigment granules that remain attached to dissected photoreceptors (Supplementary Fig. 8). These data suggest increased lysosomal storage as a result of an Atrophin-specific effect. Indeed, autofluorescent ageing pigments like lipofuscin, a product of unsaturated fatty acids oxidation associated with several lysosomal pathologies, that can be visualised by autofluorescence at 488nm[30] accumulate in large vesicles in dissected single ommatidia that express Atro75QN (Fig. 6b). Likewise, the *Drosophila* polyubiquitin binding protein Ref(2)P/p62[31], a multifunctional scaffold protein that marks ubiquitinated protein aggregates destined to degradation through the autophagic-lysosomal machinery[32] accumulates in a number of small and large bodies upon wt Atro and, more conspicuously, upon polyQ Atro overexpression (Fig. 6c).

To measure lysosomal activity as a whole we have established a biochemically amenable system based on cultured *Drosophila* BG3 cells, a neuronal line derived by larval CNS, which can be transiently transfected with an efficiency of ~20% (Supplementary Fig. 9). In addition, these cells already express endogenously Atro (Supplementary Fig. 9). Therefore, in consideration of all these properties BG3 cells constitute an ideal set up to complement and extend our *in-vivo* observations in an *in-vitro* system. Over-expression of exogenous *Atro* mutants was achieved by using the Gal4/UAS system with the same vectors (pUAST-based) used to make our DRPLA transgenic flies and a $CuSO_4$–inducible promoter present in the pMT-Gal4 plasmid (Supplementary Fig. 9).

In this neuronal cell culture we have measured bulk protein degradation upon radioactive labelling. This is the best established assay for monitoring, independently of

any substrate and of autophagy, the function of lysosomes in degrading long-lived (>4hrs half life) proteins[33]. Cells transfected with *Atro75QN* are significantly impaired or slower than control-transfected cells in degrading, after 24 hrs chase, the radioactivity present at 5 hrs chase in TCA-insoluble protein pellets (Fig. 6d). These data, taken into account the transfection efficiency, indicate a strong deficiency in degradation of long-lived proteins by the lysosomes upon expression of polyQ Atro.

Finally, in agreement with the hypothesis of lysosomal blockage, co-expression of Tor^{TED} or Atg1 with Atro75QN in the fly retina, generates gigantic electrondense autophagolysosomes with little sign of content digestion (Fig. 3a and Supplementary Fig. 6), which may explain the lack of rescue by additional induction of autophagy.

DISCUSSION

In conclusion, our study suggests that neurodegeneration in the DRPLA flies results from partial inhibition or delay of autophagic digestion that shares many similarities with lysosomal storage disorders[30,34]. We have generated new animal models for DRPLA in *Drosophila melanogaster*. The DRPLA mouse models generated in the past [35,36] have been shown to recapitulate much of the human pathology but they are less flexible and genetically amenable than *Drosophila*, which has proved to be a valuable tool for dissecting polyQ pathology[8]. Our new fly models will allow faster analysis of several aspects of DRPLA neurodegeneration also allowing detailed comparison with other polyQ disease models. Thanks to the high structural and functional conservation in the Atrophins family our observations are likely to be relevant to the human disease. In this report we focus on the cellular mechanism of degeneration and highlight the role of autophagy and the specific deregulations due to polyQ Atrophins.

Upon expression of polyQ Atrophins, autophagosomes and their markers are readily detected, in neuronal and glial cells. PolyQ proteins have been described to induce strongly autophagy[24], and this may explain the markedly increased presence of autophagic organelles upon polyQ Atrophin expression in comparison to wt Atro. However this phenotype may result as well from a block in clearance[34], making it not possible to establish the actual rate of autophagosome formation. Indeed, we report that Atrophin expression impairs lysosomal degradation, but not fusion between autophagosomes and lysosomes or correct acidification of autophagolysosomes. In photoreceptor neurons that express Atrophin mutants there is an increase in lipidic lysosomal storage as detected by autofluorescent lipofuscin pigment and an abnormal accumulation of polyubiquitinated proteins destined to be degraded by the autophagy-lysosome system, as detected by p62. Finally, neuronal *Drosophila* cells transfected with polyQ Atro are defective in degradation of the lysosomally targeted long lived proteins.

A similar accumulation of correctly acidified, yet not degradative, autophagolysosomes has also been reported to impair autophagic flux in mammalian cells as a result of incorrect maturation of the autophagolysosomes[37]. Further investigations will be required to identify the mechanism through which lysosomal digestion is impaired, however we reveal that this is an intrinsic property of Atrophin, which may account for the degenerative effect of wt Atro and may significantly modulate the toxicity of polyQ Atrophins.

Autophagy has been reported to exert a protective function in number of neurodegenerative conditions[24-27]. Consistent with these reports we find that blocking endogenous autophagy induction enhances neurodegeneration by Atrophins, as suggested by the *atg1* clones. However, we have been unable to rescue Atrophin-mediated neurodegeneration through pharmacological or genetic induction of further

autophagy. This is unique to the DRPLA flies in comparison with several other models of proteinopathies. At the ultrastructural level, further autophagy in presence of Atrophin results in the formation of gigantic autophagolysosomes with little sign of content digestion. This provides an explanation for the lack of rescue since the full autophagy cycle cannot be completed.

However, we find that blocking autophagy is also detrimental to cells undergoing neurodegeneration by Atrophins. Thus, both blocking endogenous levels of autophagy and inducing further autophagy lead to stronger or faster degeneration. This apparent paradox can be explained either by implying that autophagy is not completely blocked by polyQ Atro or that the early events leading to autophagosome formation may have themselves a protective function. Also in absence of digestion autophagosomes may indeed sequester potentially toxic material from the cytoplasm. We cannot however rigorously test these two hypotheses with currently available tools.

Important target of autophagy are damaged mitochondria, which may also contribute to cellular degeneration by Atrophins through impaired energy metabolism. Their disappearance as well as that of most cytoplasmic content in blocked autophagic vesicles may represent the final step in this form of autophagic neurodegeneration.

Autophagic degeneration by polyQ Atrophin is also induced in glial cells, where many of the observations made in photoreceptor neurons hold true. In addition to cell degeneration, expression of polyQ Atrophins in glial cells promotes pathology at the organismal level, leading to premature death, preceded by manifest locomotor deficits (data not shown). Toxicity upon glial expression is a common feature of several polyQ fly models[38,39] and, interestingly, a recent report shows that in Huntington *Drosophila* models glial cell degeneration affects fly viability, but through a different pathway than the one involved in brain neuronal toxicity[40]. Remarkably, photorecteptors are affected

by Huntingtin through the same pathway than the glia, however glial cells appear to be more sensitive to the expression of polyQ Atrophins in comparison to polyQ Huntingtin, which instead elicits a stronger effect when expressed in neurons.

The contribution of glial cells to the progression of neurodegeneration through non cell autonomous effects on neurons is an important subject of current investigations and it has been conclusively demonstrated in the case of Amyotrophic Lateral Sclerosis (ALS) and Spino Cerebellar Ataxia 7 (SCA7) [41,42]. It is likely that glial cells are crucial also for most polyQ diseases, given that polyQ proteins are expressed also in the glia. In DRPLA there is evidence that glial pathology is particularly important since intracellular aggregates have been detected in the glia and there is a significant correlation between glial cell death and degeneration of brain white matter [43,44].

An important caveat of our DRPLA flies, which applies to all *Drosophila* models of polyQ diseases, is that they are based on overexpression of mutant proteins that are known to misfold as a consequence of polyQ expansion. Many of the described phenotypes could be a consequence of this artificial condition and our results will require validation in other model organisms, under expression of mutant Atrophins at endogenous levels. However, we report important differences with respect to other polyQ fly models, which also based on overexpression of misfolded polyQ proteins, arguing for the specificity of the degenerating mechanism here described. Thus, our new DRPLA fly models will be extremely useful to further dissect the role of the autophagic flux and of glial contribution in neurodegeneration, also as a mean to explore new potential therapeutic approaches to DRPLA and related diseases.

MATERIALS AND METHODS

Genetics. The following mutant fly stocks have been used: *dEAAT1-Gal4, En-Gal4, GMR-Gal4, Rhodopsin1-Gal4, Tub-Gal4, Ptc-Gal4, Act5-Gal4, Elav-Gal4, Repo-Gal4, UAS-$_{NLS}$LacZ, UAS-GFP$_{NLS}$, UAS-dHdj1, UAS-Atg5^{IR}, UAS-Atg1^{GS10797}, UAS-DTS5-1, UAS-Htt-ex1-93Q, UAS-Tor^{TED}, UAS-Rheb, UAS-Tsc1^{IR}, UAS-GFP::Atg8a, ubi-Gal80^{ts}, atg1$^{\Delta 3D}$, Atro^{35}, Atro^{j5A3}*.

Rapamycin food. Flyfood was prepared according to our standard cornmeal recipe and DMSO or rapamycin (Sigma) dissolved 500µg/ml in DMSO was added before aliquotation in 1:500 dilutions. Flies were crossed first on standard food at 18°C, until early 1st instar larvae were visible. The adult population was then split in two and allowed to lay eggs on either DMSO or rapamycin food at 18°C. Upon pupal eclosion F1 adults were transferred at 29°C on fresh DMSO or rapamycin food and flipped in a corresponding new vial every 48 hours. Embedded eyes of the different genotypes were then sectioned and analysed in blind and in one out of three independent experiments in double blind fashion.

Molecular Cloning. DNA cloning was performed by standard techniques and by Gateway recombination system (Invitrogen). Full length or truncated *atrophin-1* cDNAs encoding the first 917 amino acids (At-1-ΔC or At-1-65QΔC) were generated by PCR using full-length human *atrophin-1* cDNAs (At-1 or At-1-65Q, a gift from David R. Borchelt) as templates, and cloned into *pUAST* to generate *UAS-At-1ΔC* and *UAS-At-1-65QΔC*. To generate *ubi-HA::At-1-ΔC*, a *At-1ΔC* cDNA was cloned into the transformation vector *pCaSpeR-UP-HA* using Gateway recombination (Invitrogen).

For *Drosophila* Atro a region containing the 65 CAG repeats of the At-1 cDNA was amplified by PCR with oligos that insert a SpeI site upstream of the CAG stretch and a BamHI site downstream of it. A XbaI-BglII 1.4kb fragment of Atro was mutagenised by PCR and Gene Tailor (Invitrogen) to introduce a SpeI and a BamHI site flanking the endogenous Q11 N-ter stretch. Upon insertion of the 65 CAG the XbaI-

BglII Atro fragment was reinserted in the pUAST-Atro plasmid to generate pUAST-Atro75QN. A 0.9kb NotI fragment of Atro was mutagenised to insert SpeI and BamHI sites flanking the C-ter region encoding for Q14 stretch. Following insertion of the 65 CAGs the NotI fragment was reinserted in the pUAST-Atro plasmid to generate pUAST-Atro66QC. Both Q stretches varied length during cloning and two comparable stretches with similar expansion were chosen. All plasmids have been sequenced at MWG Biotech. More detailed construct information is available upon request.

RNA extraction and RT-PCR. RNA was extracted from 10-20 fly heads or BG3 cell pellets using the RNAgents kit (Promega); RNA quantity and quality were assessed by Nanodrop 1000 (Thermo Scientific). 0.5µg of RNA sample was retro-transcribed with OdT or random primers and SuperScript III Reverse Transcriptase (Invitrogen) to generate cDNAs which were used as PCR templates. For qPCR we used SYBR Green JumpStart Taq ReadyMix (Sigma) and 500nM of specific primers for *at-1* and *rp49*. Amplification and *at-1* vs *rp49* quantification was performed on an IQ5 (BioRad). Sequences of all oligos are available upon request.

Histology and Electron Microscopy. For retinal semithin sections adult heads were treated and sectioned as previously described[45]. For EM sections adult heads were dissected and fixed at RT in 4% PFA; 2% glutaraldehyde in 0.12M sodium cacodylate buffer at pH 7.4 for 1hr. The heads were then washed 3 x 10min in 0.12M sodium cacodylate buffer, post-fixed in 2% OsO4 in 0.12M sodium cacodylate buffer for 1hr and washed again 3 x 10min. Afterwards, samples were dehydrated in ethanol series and infiltrated with propylene oxide, embedded in epoxy resin (Fluka) and polymerized at 80°C. Ultrathin (80 nm) plastic sections were cut on a Leica UltraCut microtome using a diamond Diatome knife and post stained with 2% uranyl acetate, followed by Reynolds' lead citrate, and stabilized for transmission electron microscopy by carbon coating. Examination was performed with a Zeiss Leo 912 microscope at 100 kV.

Images were captured with a Gatan 792 Bioscan camera using Digital Micrograph as software.

Immunohistochemistry. Larval imaginal discs and brains were treated as previously described[45].

For Lysotracker staining wing imaginal discs from third instar larvae were dissected in PBS and stained with LysoTracker Red DND-99 (Molecular Probes) diluted 1:1000 in PBS for 10 s after 3 min of fixation in 3% formaldehyde (Polysciences Inc.). Mounting was performed in Vectashield and samples were immediately visualized by fluorescent microscopy.

Immunostainings of adult retina were performed with whole-mount preparation. Staged eyes were dissected and fixed in 4% formaldehyde in PBS for 1hr. The brain was removed approximately 30min into fixation. Fixed eyes were then given three 10min washes in PBST (PBS plus 0.3% Triton X-100). Washed eyes were incubated in primary antibody in PBST plus 5% goat serum overnight at 4°C. Eyes were given three 10min washes in PBST and incubated for 4hr at RT in secondary antibody followed by an overnight staining in 2 mg/ml rhodamine-conjugated phalloidin (Sigma). After incubation, eyes were given three 10min PBST washes and mounted in Vectashield.

TUNEL staining in fixed imaginal discs and adult retinae was performed with the DeadEnd kit (Promega), according to the protocol from the supplier.

Single ommatidia were dissected adapting a protocol by R.C. Hardie[46]. Briefly, adult retinae were grossly dissected in Schneider's insect medium supplemented with 10% Fetal Calf Serum. The dissected retina were then transferred in a drop of fresh new Schneider's medium with 10% FCS on a glass slides and ommatidia were dissected with fine forceps. At this point LysoTracker Red DND-99 (Molecular Probes) was added if required, and then most of the medium was removed with a pipette before

adding Vectashield and sealing with a coverslip. All samples were imaged within 24 hours.

Antibodies used: goat anti-human Atrophin-1 APG840 (1/500)[18], rat anti-Elav (1/10) (hybridoma-supernatant 7E8A10 from DSHB), mouse anti-Repo (1/10) (8D12 Hybridoma Bank), rabbit anti-β-galactosidase (1/1000) (Cappel ICN-Pharmaceuticals Inc.), mouse anti-HA (1/1000) (16B12 Covance), rabbit anti-GFP (1:500, Molecular Probe), rabbit anti-Atro (1/500), rabbit anti-p62 (1/2000) (a gift from Didier Contamine) mouse anti-HSP70 (1/500) (MA3-007, Affinity BioReagents), mouse anti-ubiquitin (1/200) (13-1600, Zymed), mouse anti-TBP (1/200) (sc-421, Santa Cruz), rabbit anti-Nervy (1/300) (a gift from Richard S.Mann)**,** rabbit anti-Sin3A (1/200) and rabbit anti-RPD3 (1/200) (a gift from Lori Pile), and rabbit anti-Mi2 (1/500) (a gift from Alexander Brehm), mouse anti-PolyQ (1/200)(IC2, Chemicon). Secondary fluorescence-conjugated antibodies from Molecular Probes or Jackson Laboratories were used at 1:200 dilutions. Samples were viewed with Zeiss AxioplanII, BioRad and Zeiss LSM confocal microscopes.

Western Blots. For flies, 10 fly heads were dissected, mashed directly in Laemmli buffer and boiled at 95°C for 5 min. For cells, a T25 flask was harvested, pelleted and resuspended in Laemmli buffer. Polyacrylammide gels, blotting and antibody staining were performed according to standard protocols. Amersham ECL reagents where used for chemiluminescence. Primary antibodies used: anti-human Atrophin-1 APG840 (1/500) and anti-Atro (1/200).

Cell Cultures and metabolic labelling. Neuronal BG3 cells (clone 1) were obtained from the Drosophila Genomics Resource Center and cultured in flasks with Shields and Sang M3 Insect Medium (Sigma) supplemented with 10%FCS (Gibco), PenStrep and Insulin. For the highest transfection efficiency (~20%) we used the Effectene kit (Qiagen).

For radioactive metabolic labelling, cells at 50-70% confluence were transiently transfected with Endofree purified (Qiagen) Copper-inducible pMT-Gal4 and a molar excess (2 folds) of UAS vectors (pUAST or pUAST-Atro75QN). After 24 hours with the transfection medium, each flask of cells was incubated for 48 hours in radioactive medium containing 12.5MBq of EasyTag EXPRE^{35}S^{35}S mix (Perkin Elmer) and 1mM $CuSO_4$. Thereafter cells were incubated for 5 or 24 hours with chase medium containing 1mM $CuSO_4$, then harvested and lysed in PBS + 1% Tx-100. Proteins were precipitated with 10% Trichloroacetic Acid (TCA) and resuspended in Laemmli buffer. Samples were loaded onto a 10% SDS-PAGE gel, the gel was dried and exposed to a phosphoimager screen. Signals were scanned with a Thyphoon 8600 (Molecular Dynamics) and volumetrically quantified by ImageQuant software. The radioactivity for each TCA pellet was standardised over the radioactivity present in the chase medium as secreted proteins which escape intracellular degradation. Finally, with these standardised values, the 24hr/5hr ratio was established for each transfection in each experiment according to the formula $r=(P_{24hr}/M_{24hr}):(P_{5hr}/M_{5hr})$.

Supplementary Information accompanies the paper on the Cell Death and Differentiation website (http://www.nature.com/cdd)

Acknowledgements We thank Gabriele Schilling, David Borchelt, Helen McNeill, Joe Bateman, Tor Erik Rusten, Serge Birman, Thomas Neufeld, the DHSB, DGRC and Bloomington for reagents and stocks, Aïcha Ouane for technical assistance, Joy Burchell and Steve Catchpole for help with the phosphoimager. M.F. is supported by the Italian Telethon Foundation with a career development award and is an Assistant Telethon Scientist. This work was also supported by the European Union Marie Curie European Reintegration Grant 505739, by Fondazione Cariplo and Compagnia di San Paolo grants to M.F and funds from the Centre National de la Recherche Scientifique to B.C. and the KCL School of Biomedical and Health Sciences to M.F.

REFERENCES

1. Ross CA. Polyglutamine pathogenesis: emergence of unifying mechanisms for Huntington's disease and related disorders. Neuron. 2002;35:819-822.
2. Arrasate M, Mitra S, Schweitzer ES, Segal MR, Finkbeiner S. Inclusion body formation reduces levels of mutant huntingtin and the risk of neuronal death. Nature. 2004;431:805-810.
3. Mizushima N, Levine B, Cuervo AM, Klionsky DJ. Autophagy fights disease through cellular self-digestion. Nature. 2008;451:1069-1075.
4. Nixon RA. Autophagy in neurodegenerative disease: friend, foe or turncoat? Trends in neurosciences. 2006;29:528-535.
5. Chen HK, Fernandez-Funez P, Acevedo SF, Lam YC, Kaytor MD, Fernandez MH, et al. Interaction of Akt-phosphorylated ataxin-1 with 14-3-3 mediates neurodegeneration in spinocerebellar ataxia type 1. Cell. 2003;113:457-468.
6. Emamian ES, Kaytor MD, Duvick LA, Zu T, Tousey SK, Zoghbi HY, et al. Serine 776 of ataxin-1 is critical for polyglutamine-induced disease in SCA1 transgenic mice. Neuron. 2003;38:375-387.
7. Warrick JM, Morabito LM, Bilen J, Gordesky-Gold B, Faust LZ, Paulson HL, et al. Ataxin-3 suppresses polyglutamine neurodegeneration in Drosophila by a ubiquitin-associated mechanism. Mol Cell. 2005;18:37-48.
8. Marsh JL, Thompson LM. Drosophila in the study of neurodegenerative disease. Neuron. 2006;52:169-178.
9. Romero E, Cha GH, Verstreken P, Ly CV, Hughes RE, Bellen HJ, et al. Suppression of neurodegeneration and increased neurotransmission caused by expanded full-length huntingtin accumulating in the cytoplasm. Neuron. 2008;57:27-40.
10. Naito H, Oyanagi S. Familial myoclonus epilepsy and choreoathetosis: hereditary dentatorubral-pallidoluysian atrophy. Neurology. 1982;32:798-807.
11. Nagafuchi S, Yanagisawa H, Ohsaki E, Shirayama T, Tadokoro K, Inoue T, et al. Structure and expression of the gene responsible for the triplet repeat disorder, dentatorubral and pallidoluysian atrophy (DRPLA). Nature genetics. 1994;8:177-182.
12. Erkner A, Roure A, Charroux B, Delaage M, Holway N, Core N, et al. Grunge, related to human Atrophin-like proteins, has multiple functions in Drosophila development. Development. 2002;129:1119-1129.
13. Shen Y, Lee G, Choe Y, Zoltewicz JS, Peterson AS. Functional architecture of atrophins. J Biol Chem. 2007;282:5037-5044.
14. Zhang S, Xu L, Lee J, Xu T. Drosophila atrophin homolog functions as a transcriptional corepressor in multiple developmental processes. Cell. 2002;108:45-56.
15. Zoltewicz JS, Stewart NJ, Leung R, Peterson AS. Atrophin 2 recruits histone deacetylase and is required for the function of multiple signaling centers during mouse embryogenesis. Development. 2004;131:3-14.
16. Charroux B, Freeman M, Kerridge S, Baonza A. Atrophin contributes to the negative regulation of epidermal growth factor receptor signaling in Drosophila. Dev Biol. 2006;291:278-290.
17. Nucifora FC, Jr., Ellerby LM, Wellington CL, Wood JD, Herring WJ, Sawa A, et al. Nuclear localization of a non-caspase truncation product of atrophin-1, with an

expanded polyglutamine repeat, increases cellular toxicity. J Biol Chem. 2003;278:13047-13055.
18. Wood JD, Nucifora FC, Jr., Duan K, Zhang C, Wang J, Kim Y, et al. Atrophin-1, the dentato-rubral and pallido-luysian atrophy gene product, interacts with ETO/MTG8 in the nuclear matrix and represses transcription. J Cell Biol. 2000;150:939-948.
19. Karres JS, Hilgers V, Carrera I, Treisman J, Cohen SM. The conserved microRNA miR-8 tunes atrophin levels to prevent neurodegeneration in Drosophila. Cell. 2007;131:136-145.
20. Steffan JS, Bodai L, Pallos J, Poelman M, McCampbell A, Apostol BL, et al. Histone deacetylase inhibitors arrest polyglutamine-dependent neurodegeneration in Drosophila. Nature. 2001;413:739-743.
21. Holmberg CI, Staniszewski KE, Mensah KN, Matouschek A, Morimoto RI. Inefficient degradation of truncated polyglutamine proteins by the proteasome. The EMBO journal. 2004;23:4307-4318.
22. Venkatraman P, Wetzel R, Tanaka M, Nukina N, Goldberg AL. Eukaryotic proteasomes cannot digest polyglutamine sequences and release them during degradation of polyglutamine-containing proteins. Mol Cell. 2004;14:95-104.
23. Scott RC, Schuldiner O, Neufeld TP. Role and regulation of starvation-induced autophagy in the Drosophila fat body. Dev Cell. 2004;7:167-178.
24. Ravikumar B, Vacher C, Berger Z, Davies JE, Luo S, Oroz LG, et al. Inhibition of mTOR induces autophagy and reduces toxicity of polyglutamine expansions in fly and mouse models of Huntington disease. Nature genetics. 2004;36:585-595.
25. Berger Z, Ravikumar B, Menzies FM, Oroz LG, Underwood BR, Pangalos MN, et al. Rapamycin alleviates toxicity of different aggregate-prone proteins. Hum Mol Genet. 2006;15:433-442.
26. Sarkar S, Krishna G, Imarisio S, Saiki S, O'Kane CJ, Rubinsztein DC. A rational mechanism for combination treatment of Huntington's disease using lithium and rapamycin. Hum Mol Genet. 2008;17:170-178.
27. Wang T, Lao U, Edgar BA. TOR-mediated autophagy regulates cell death in Drosophila neurodegenerative disease. J Cell Biol. 2009.
28. Scott RC, Juhasz G, Neufeld TP. Direct induction of autophagy by Atg1 inhibits cell growth and induces apoptotic cell death. Curr Biol. 2007;17:1-11.
29. Degtyarev M, De Maziere A, Orr C, Lin J, Lee BB, Tien JY, et al. Akt inhibition promotes autophagy and sensitizes PTEN-null tumors to lysosomotropic agents. J Cell Biol. 2008;183:101-116.
30. Venkatachalam K, Long AA, Elsaesser R, Nikolaeva D, Broadie K, Montell C. Motor deficit in a Drosophila model of mucolipidosis type IV due to defective clearance of apoptotic cells. Cell. 2008;135:838-851.
31. Nezis IP, Simonsen A, Sagona AP, Finley K, Gaumer S, Contamine D, et al. Ref(2)P, the Drosophila melanogaster homologue of mammalian p62, is required for the formation of protein aggregates in adult brain. J Cell Biol. 2008;180:1065-1071.
32. Bjorkoy G, Lamark T, Brech A, Outzen H, Perander M, Overvatn A, et al. p62/SQSTM1 forms protein aggregates degraded by autophagy and has a protective effect on huntingtin-induced cell death. J Cell Biol. 2005;171:603-614.
33. Cuervo AM, Dice JF, Knecht E. A population of rat liver lysosomes responsible for the selective uptake and degradation of cytosolic proteins. J Biol Chem. 1997;272:5606-5615.

34. Settembre C, Fraldi A, Jahreiss L, Spampanato C, Venturi C, Medina D, et al. A block of autophagy in lysosomal storage disorders. Hum Mol Genet. 2008;17:119-129.
35. Sato T, Miura M, Yamada M, Yoshida T, Wood JD, Yazawa I, et al. Severe neurological phenotypes of Q129 DRPLA transgenic mice serendipitously created by en masse expansion of CAG repeats in Q76 DRPLA mice. Hum Mol Genet. 2009;18:723-736.
36. Schilling G, Wood JD, Duan K, Slunt HH, Gonzales V, Yamada M, et al. Nuclear accumulation of truncated atrophin-1 fragments in a transgenic mouse model of DRPLA. Neuron. 1999;24:275-286.
37. Razi M, Chan EY, Tooze SA. Early endosomes and endosomal coatomer are required for autophagy. J Cell Biol. 2009;185:305-321.
38. Tamura T, Sone M, Yamashita M, Wanker EE, Okazawa H. Glial cell lineage expression of mutant ataxin-1 and huntingtin induces developmental and late-onset neuronal pathologies in Drosophila models. PloS one. 2009;4:e4262.
39. Kretzschmar D, Tschape J, Bettencourt Da Cruz A, Asan E, Poeck B, Strauss R, et al. Glial and neuronal expression of polyglutamine proteins induce behavioral changes and aggregate formation in Drosophila. Glia. 2005;49:59-72.
40. Lievens JC, Iche M, Laval M, Faivre-Sarrailh C, Birman S. AKT-sensitive or insensitive pathways of toxicity in glial cells and neurons in Drosophila models of Huntington's disease. Hum Mol Genet. 2008;17:882-894.
41. Custer SK, Garden GA, Gill N, Rueb U, Libby RT, Schultz C, et al. Bergmann glia expression of polyglutamine-expanded ataxin-7 produces neurodegeneration by impairing glutamate transport. Nat Neurosci. 2006;9:1302-1311.
42. Boillee S, Vande Velde C, Cleveland DW. ALS: a disease of motor neurons and their nonneuronal neighbors. Neuron. 2006;52:39-59.
43. Hayashi Y, Kakita A, Yamada M, Koide R, Igarashi S, Takano H, et al. Hereditary dentatorubral-pallidoluysian atrophy: detection of widespread ubiquitinated neuronal and glial intranuclear inclusions in the brain. Acta neuropathologica. 1998;96:547-552.
44. Yamada M, Sato T, Tsuji S, Takahashi H. Oligodendrocytic polyglutamine pathology in dentatorubral-pallidoluysian atrophy. Ann Neurol. 2002;52:670-674.
45. Montrasio S, Mlodzik M, Fanto M. A new allele uncovers the role of echinus in the control of ommatidial rotation in the Drosophila eye. Dev Dyn. 2007;236:2936-2942.
46. Hardie RC. Voltage-sensitive potassium channels in Drosophila photoreceptors. J Neurosci. 1991;11:3079-3095.

Figure 1. Neuronal degeneration by polyglutamine Atrophins. Ageing in all figures was done at 29°C. **a,** Schematic representations of fly Atro and human Atrophin-1 protein architecture and polyglutamine expansions. **b,** Eye pictures of 1 month old flies expressing different forms of *Drosophila* Atro and of human Atrophins with *GMR-Gal4*. Eye depigmentation is visible especially in

GMR>Atro75QN and in *GMR>At-1-65QΔC*. **c,** Tangential eye sections at the dorso-ventral midline of flies expressing different forms of Atro with *Rh1-Gal4*. Photoreceptor loss is observed in with all Atro forms after 35 days, more severe with Atro66QC and Atro75QN (See Supplementary Fig.1 for quantification). White arrows point at intact R7 cells in ommatidia that have lost all or most other photoreceptors. The *Rh1* driver is not expressed in R7/R8.

Figure 2. Glial and neuronal toxicity of Atrophins. a, Viability curves for flies expressing specifically in the adult life different forms of *Drosophila* Atro in the glia with the *dEAAT1* driver. Adult expression has been achieved thanks to the Gal80 repressor carrying a temperature sensitive mutation. **b,** Viability curves for flies expressing specifically in the adult life different forms of *Drosophila* Atro in neurons with the *Elav* driver. **c,** Viability curve of flies expressing different *Drosophila* Atro proteins in the glia. Atro75QN strongly reduces viability whereas Atro66QC only causes a modest but significant (Kaplan Mayer Log Rank 30.95, $p<0.0001$) reduction with respect to control flies. **d,** Viability curves of flies expressing At-1-65Q in the glia with the *dEAAT1* driver either alone or in combination with Tor^{TED}. Tor^{TED} brings about a significant enhancement of fly mortality (Kaplan Mayer Log Rank 93.42, $p<0.0001$). **e,** Viability curve of flies expressing different human At-1 forms in the glia with the *dEAAT1* driver. At-1-65QΔC strongly reduces viability with respect to control flies, At-1-65Q causes a modest but significant reduction (Kaplan Mayer Log Rank 16.52, $p<0.0001$) and full length At-1 improves viability. **f,** Viability curves for flies expressing different human At-1 forms in neurons with the *Elav* driver. Only At-1-65QΔC reduces viability significantly with repect to control flies.

Figure 3. Autophagy in the DRPLA fly models. a, EM retinal pictures of control flies or flies expressing different Atro forms and or Tor^{TED} with the *GMR* driver and aged 14d. Arrowheads point at autophagosomes (also shown in the top left zoom inset in the Atro wt panel), arrows at large autophagolysosomes that become gigantic with Tor^{TED}. Control flies display a virtually intact tissue, whereas expression of Tor^{TED} brings about the formation of large vacuoles that appear empty (arrowhead). Zoom in panels show (top to bottom) a multilamellar body, autophagosomes with undigested material and a damaged mitochondrion. Scale bars 2μm, except Atro75QN + Tor^{TED} 5μm. **b,** Confocal pictures of whole-mount retinae of flies expressing with *GMR* different Atro forms and GFP::Atg8a, aged 10d. Red is phalloidin marking rhabdomeres, green is GFP. Accumulation of small GFP::Atg8a dots is mostly in non-neuronal interommatidial cells with wt Atro. Atro66QC and Atro75QN cause the GFP signal to gather in large amasses also inside photoreceptors (arrows). R7 photoreceptors are marked unspecifically for a technical artefact. Scale bars 2μm.

Figure 4. Modulation of autophagy does not rescue cell degeneration. a, Tangential eye sections through $atg1^{\Delta 3D}$ clones (marked by the absence of yellow pigment) in flies either *wt* or expressing Atro75QN with *GMR* and aged 14d. Many ommatidia display severely reduced complement of photoreceptors specifically inside clones in Atro75QN expressing flies (arrow). Only occasional photoreceptor loss is present inside clones in the *wt* background (arrowhead). **b,** Histograms showing the number of photoreceptors (PR) of *GMR>Atro75QN/* $Tor^{\Delta P}$ flies on 1μM rapamycin food aged for 2 or 7 days. The 2 days chart represents blind counts of 1681 ommatidia (24 flies) for DMSO controls and

2514 ommatidia (34 flies) for rapamycin from three independent experiments, Chi-square value is 36.5; $p<0.001$ for 6 degrees of freedom. The chart at 7 days represents 679 ommatidia (10 flies) for DMSO and 608 ommatidia (9 flies) for rapamycin from two independent experiments, Chi-square 77.9; $p<0.001$.

Figure 5. Genetic modifiers of retinal degeneration. a, Horizontal head section of a wt fly at the dorso-ventral midline. Arrows show the extent of the retina (r) and of the medulla (m). **b,** Horizontal head sections of flies overexpressing different forms of *Drosophila* Atro and/or other transgenes with the *GMR* driver. Sections are representative examples for each genotype and the ratio ± standard deviation of the extent of the retina over the underlying medulla is reported in each panel. The medulla is unaffected by *GMR* expression and is a control for unspecific fly size effect. Flies were allowed to develop at 18°C and newly eclosed adults were aged at 29°C for 28 days. On average six female heads coming from 2-3 independently aged populations were sectioned for each genotype. In the top row, all Atro proteins cause a highly significant ($p<0.001$) degeneration of the retinal tissue compared to control flies (*GMR-Gal4*, left most). For genetic interactions with other mutants, statistically significant changes (two tailed t-test, $p<0.05$) in comparison to the w^{1118} negative control (first line of the corresponding column) are in red. **c,** Horizontal head sections of flies overexpressing different forms of human Atrophins with *GMR-Gal4*. Only At-1-65QΔC causes a significant decrease in the extent of the retina, whereas At-1-65Q does not display an effect in this assay, despite the same 65Q expansion.

Figure 6. Lysosomal impairement by Atrophins. a, Single ommatidia dissected from flies expressing GFP::Atg8 with *GMR-Gal4* alone or in the presence of Atro wt or Atro75QN, aged 14 days. GFP fluorescence is in green, Lysotracker to mark acid lysosomes in red. Arrows point at some of the many autophagolysosomes correctly formed which appear yellow. Note that the small bright red dots are pigment granules (see Supplementary Fig. 8). Scale bars 2μm. **b,** Single ommatidia dissected from control flies or flies expressing Atro75QN with *GMR-Gal4*, aged 14 days. Arrows point at large vesicles of autofluorescent lipofuscin pigment detected at 488 nm. Small dots also found in control ommatidia are pigment granules. Scale bars 2μm. **c,** Confocal pictures of whole-mount retinae of flies expressing with *GMR* different Atro forms, aged 10d. Red is phalloidin marking rhabdomeres, blue is p62. Atro wt and, more prominently, Atro66QC and Atro75QN cause accumulation of p62 in large amasses (arrows). Scale bars 2μm. **d,** Histograms showing the ratio between the ^{35}S radioactivity signal incorporated in acid insoluble proteins after 24 hours chase with respect to 5 hours chase. BG3 neuronal cells were co-transfected with either a control pUAST plasmid or with pUAST-Atro75QN together with pMT-Gal4. Short-lived proteins, mainly degraded by the proteasome, do not contribute to the signal as they are eliminated before 5 hours chase. The quantified signal has also been standardised for any radioactive proteins present in the chase medium which may contribute to the signal but escape intracellular degradation. * indicates $p<0.05$ in two tails t-test.

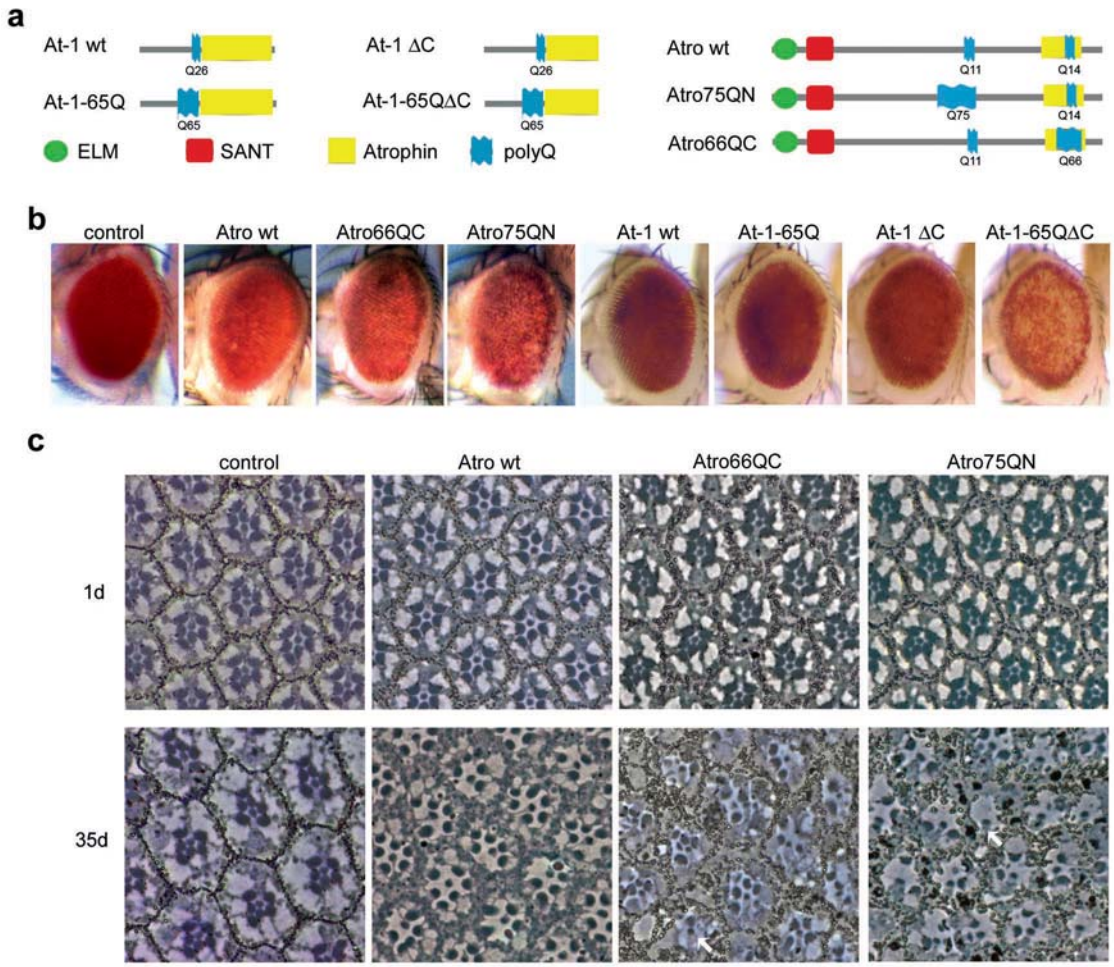

Nisoli *et al.* Fig. 1

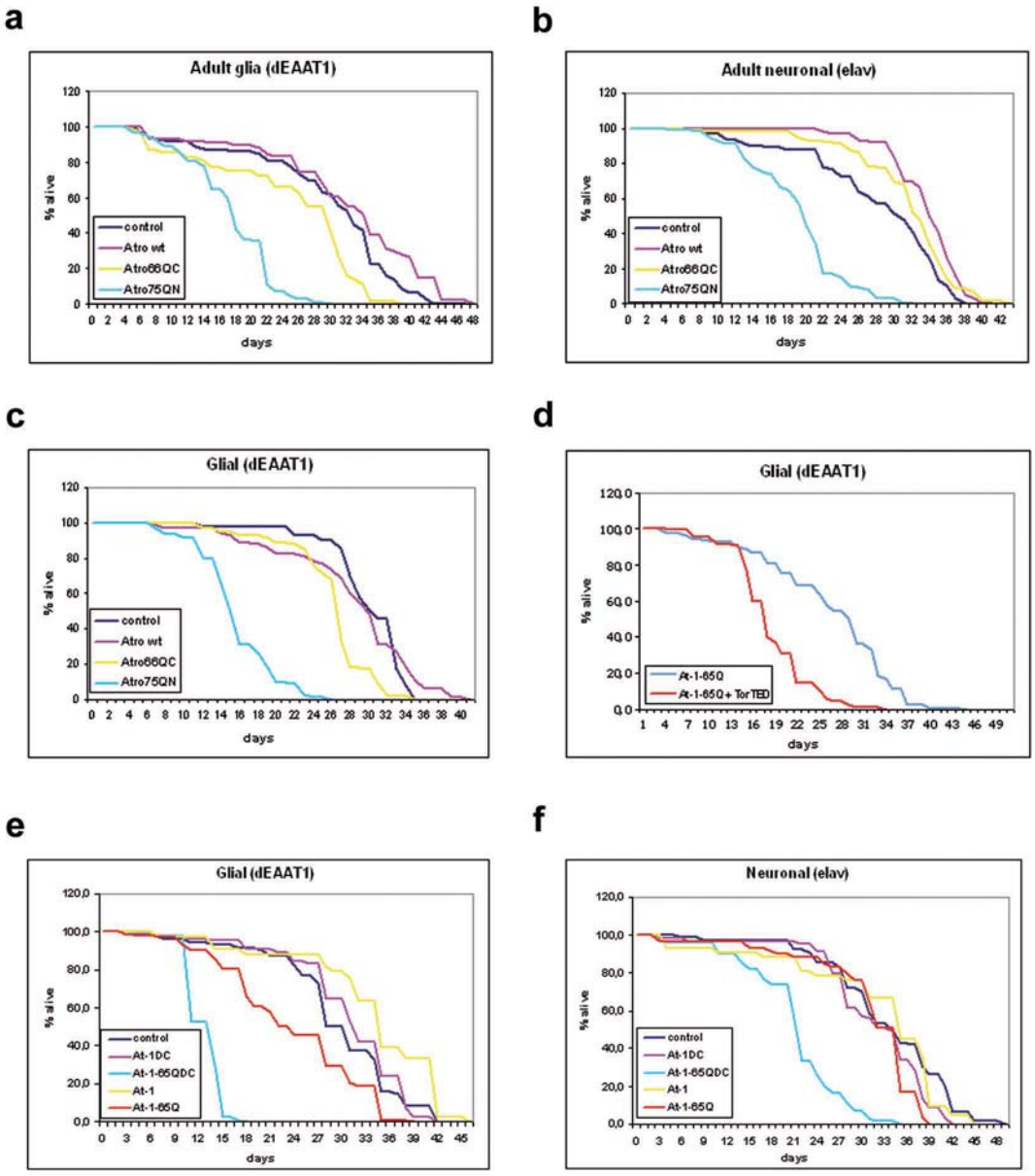

Nisoli *et al.* Fig. 2

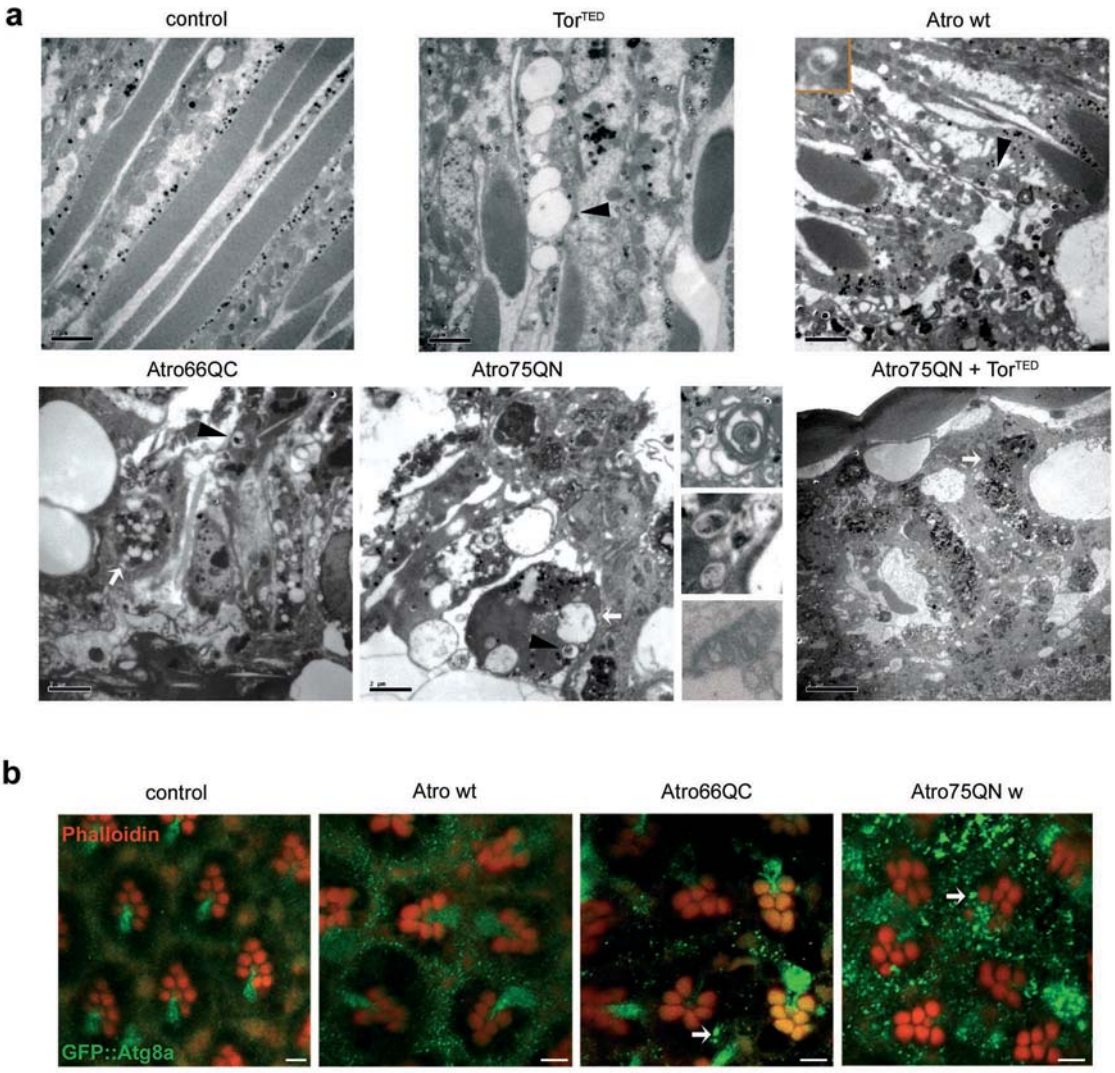

Nisoli *et al.* Fig. 3

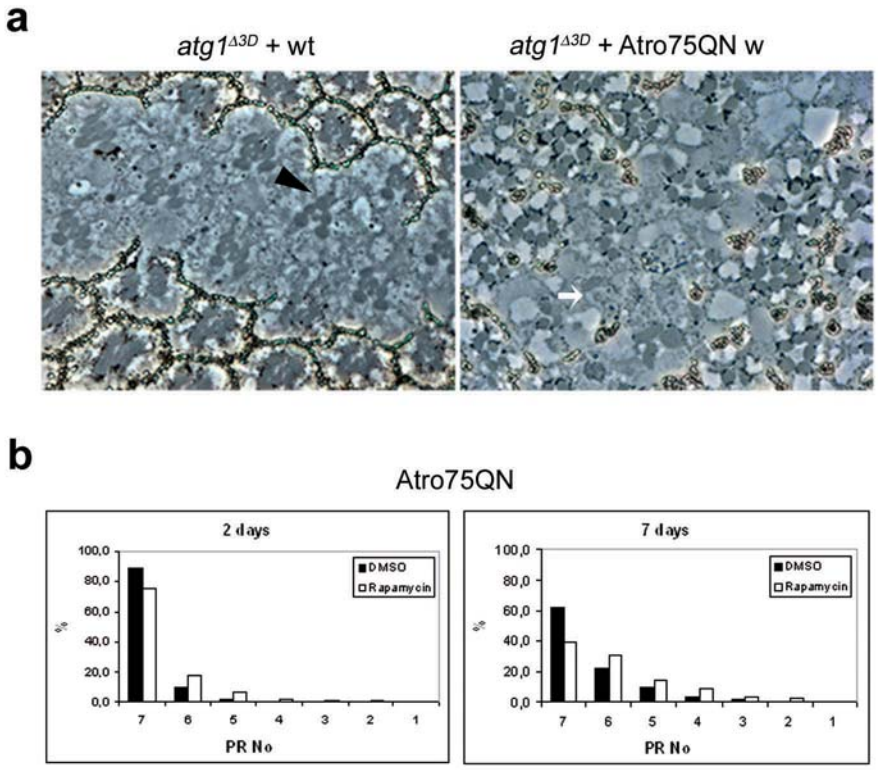

Nisoli *et al.* Fig. 4

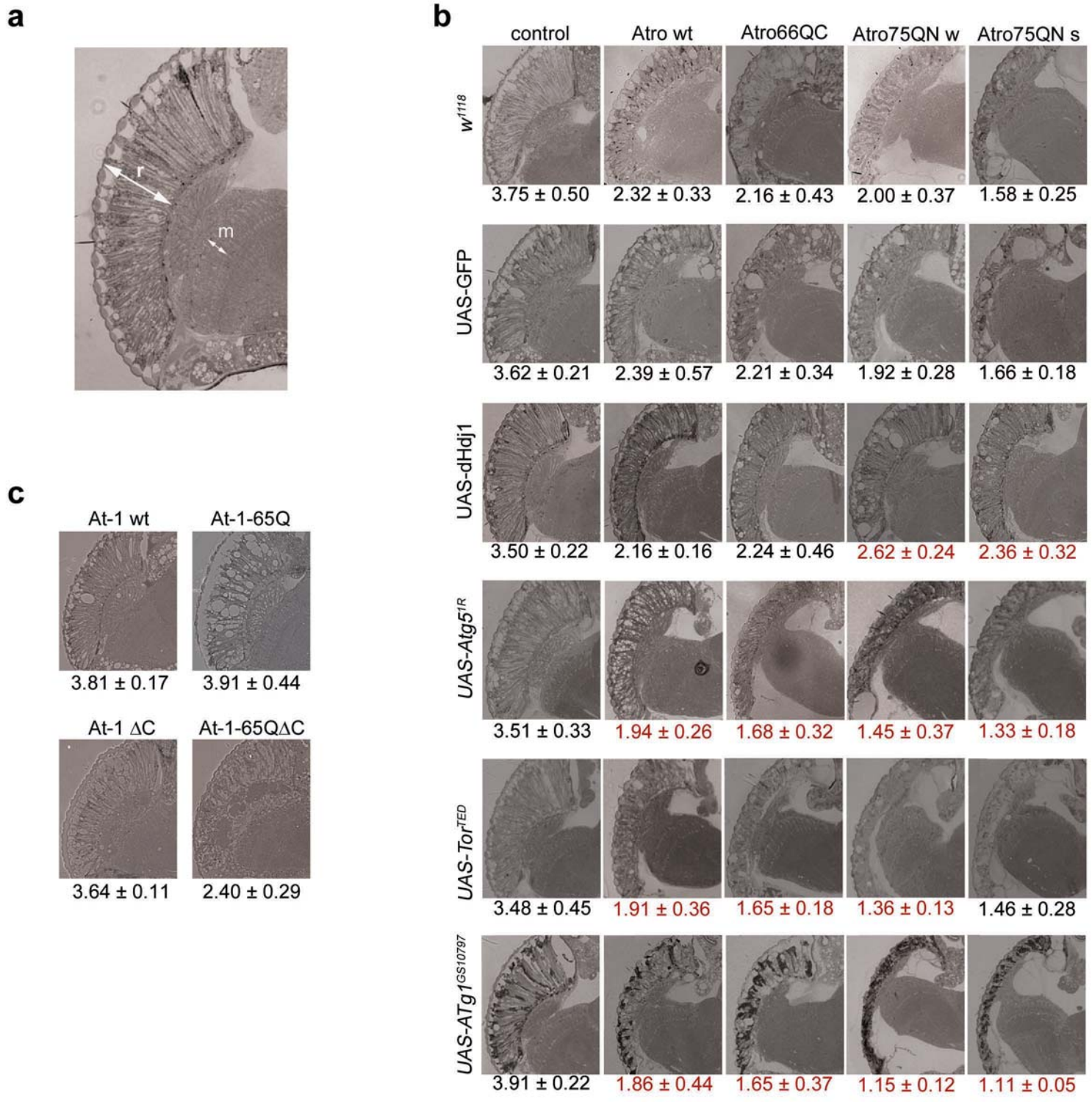

Nisoli *et al.* Fig. 5

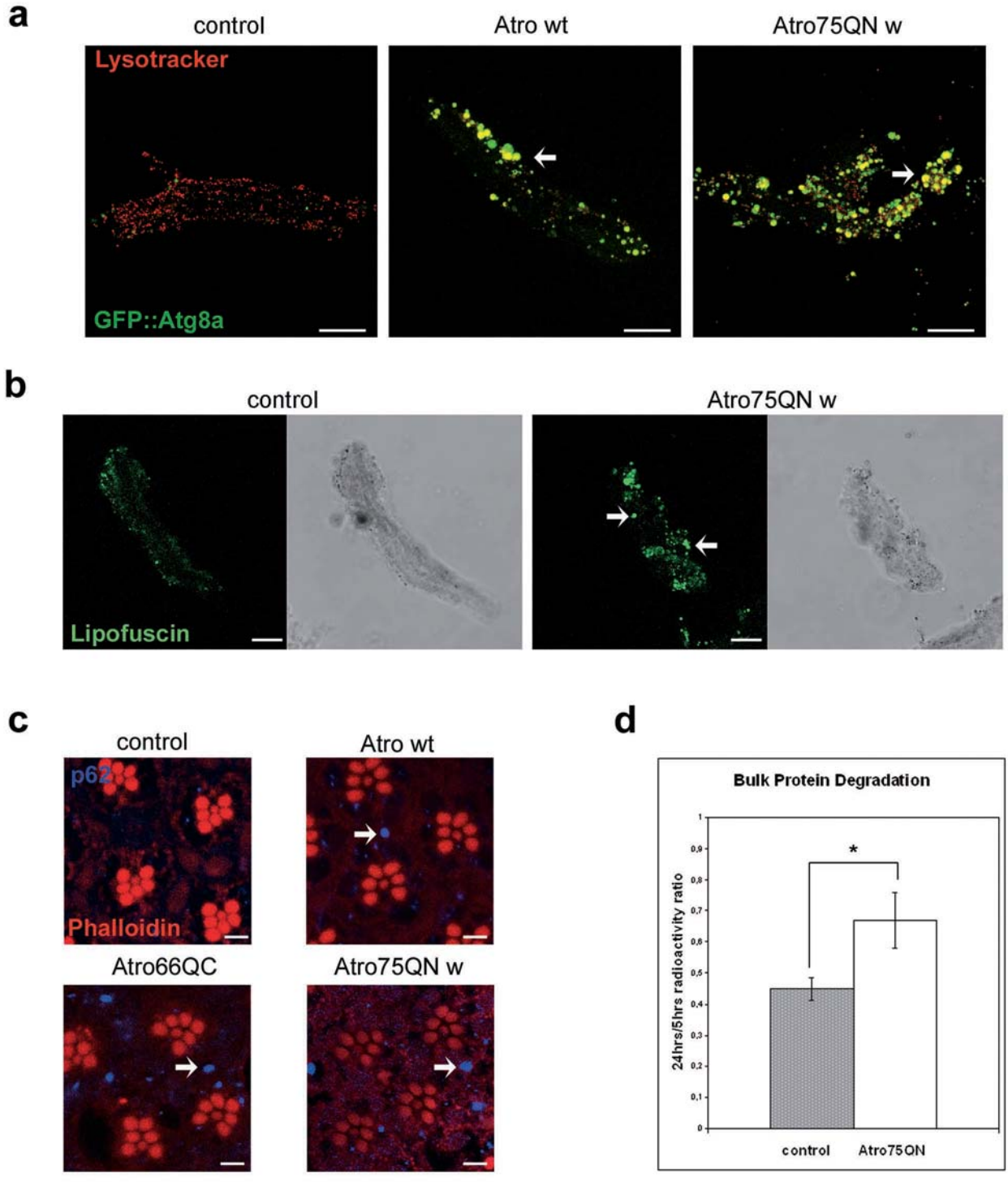

Nisoli *et al.* Fig. 6